

Authority NASA PUBLICATIONS
ANNOUNCEMENTS NO.
Date

Copy /

RM SA54B16

APR 10 1954 REC'D

Source of Acquisition
CASI Acquired

PERMANENT FILE COPY

~~CLASSIFICATION~~

Authority NASA PUBLICATIONS
ANNOUNCEMENTS NO. 7
Date 6/30/59 by

~~CONFIDENTIAL~~
NACA

NACA RM 54-416

Restriction/Classification
Cancelled

~~CONFIDENTIAL~~
BLE

RESEARCH MEMORANDUM

for the

United States Air Force

EFFECT OF A LEADING-EDGE FLAP UPON THE LIFT, DRAG, AND

PITCHING MOMENT OF AN AIRPLANE EMPLOYING

A THIN, UNSWEPT WING

By John C. Heitmeyer

Ames Aeronautical Laboratory
Moffett Field, Calif.

~~CONFIDENTIAL~~

~~CONFIDENTIAL~~
John C. Heitmeyer 10/10/54
Ames Aeron. Research
NACA

JCH NACA change # 2734
~~CONFIDENTIAL~~

This material contains information affecting the National Defense of the United States within the meaning of the Espionage Laws, Title 18, U.S.C., Sec. 793 and 794, and the transmission or revelation of which in any manner to an unauthorized person is prohibited by law.

NATIONAL ADVISORY COMMITTEE
FOR AERONAUTICS
WASHINGTON

FILE COPY

To be returned to
the files of the National
Advisory Committee
for Aeronautics
Washington, D. C.

Feb. 16, 1954

~~CONFIDENTIAL~~
~~CONFIDENTIAL~~
CLASSIFIED
DATE 10/10/54 BY

14

NATIONAL ADVISORY COMMITTEE FOR AERONAUTICS

RESEARCH MEMORANDUM

for the

United States Air Force

EFFECT OF A LEADING-EDGE FLAP UPON THE LIFT, DRAG, AND

PITCHING MOMENT OF AN AIRPLANE EMPLOYING

A THIN, UNSWEPT WING

By John C. Heitmeyer

SUMMARY

The effects of deflecting full-span, constant-chord, leading-edge flaps, having either round or sharp leading edges, upon the lift, drag, and pitching-moment characteristics of a model of an interceptor-type aircraft have been determined experimentally at subsonic and supersonic speeds. Results indicate that the variations of lift with angle of attack and of pitching moment with lift were unaffected by either the shape of the flap leading edge or flap deflection. Deflection of the flaps having either a round or sharp leading edge increased the drag at zero lift at both subsonic and supersonic speeds. In spite of the increase in the drag at zero lift, however, deflection of the flaps increased the maximum lift-drag ratio at subsonic speeds and had no deleterious effect at supersonic speeds.

INTRODUCTION

At subsonic speeds, camber is effective in improving the drag characteristics of thin airfoils at angles of attack. Symmetrical wings can be cambered by deflection of a leading-edge flap. Hence, an investigation of the effects of leading-edge flaps upon the lift, drag, and pitching-moment characteristics was included in the test program of a model of an interceptor-type aircraft conducted at subsonic and supersonic speeds in the Ames 6- by 6-foot supersonic wind tunnel. The model employed an unswept wing of aspect ratio 2.50, which was fitted with sealed, full-span, constant-chord, leading-edge flaps. To determine the influence of the nose shape of the leading-edge flap, two wings, both 3.4-percent thick, were investigated; one wing had a circular-arc biconvex section, the other a rounded nose section.

NOTATION

The lift, drag, and pitching-moment characteristics are referred to the stability axis with the origin located at the quarter-chord point of the mean aerodynamic chord projected to the fuselage center line.

b	wing span
c	local wing chord
\bar{c}	mean aerodynamic chord, $\frac{\int_0^{b/2} c^2 dy}{\int_0^{b/2} c dy}$
C_D	drag coefficient, $\frac{\text{drag}}{qS}$
C_L	lift coefficient, $\frac{\text{lift}}{qS}$
C_m	pitching-moment coefficient, $\frac{\text{pitching moment}}{qSc}$
$\frac{L}{D}$	lift-drag ratio
$\left(\frac{L}{D}\right)_{\text{max}}$	maximum lift-drag ratio
M	Mach number
q	free-stream dynamic pressure
R	Reynolds number based on mean aerodynamic chord
S	total projected wing area including area formed by extending the leading and trailing edges to plane of symmetry
y	perpendicular distance from plane of symmetry
α	angle of attack of longitudinal axis, deg
δ	angle between wing chord plane and flap chord plane measured perpendicular to flap hinge line, positive for upward deflection with respect to wing, deg

APPARATUS AND PROCEDURE

Wind Tunnel and Balance

The experimental investigation was conducted in the Ames 6- by 6-foot supersonic wind tunnel. In this wind tunnel, the test Mach number can be varied continuously from 0.60 to 0.90 and from 1.20 to 1.90, and the stagnation pressure can be regulated to maintain a given test Reynolds number.

The models were sting mounted in the wind tunnel. The pitch plane of the model was horizontal. A 2-1/2-inch-diameter, six-component, flexure-pivot balance, enclosed within the body of the model, measured the aerodynamic forces and moments experienced by the model.

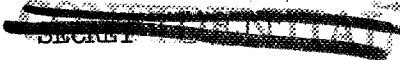
Model

The model is shown in plan and front views, together with pertinent model dimensions in figure 1. The airfoil section of each of the wings considered in the present investigation is illustrated in figure 2. The sharp-nose airfoil was a 3.4-percent-thick biconvex section, while the forward half of the round-nose section was a semi-ellipse which, for the thickness ratios considered, resembles closely an NACA 66-00X airfoil section.

Each wing panel was fitted with a full-span, constant-chord, leading-edge flap having a streamwise chord equal to 11.7 percent of the wing mean aerodynamic chord, and an area equal to 4 percent of the total wing area. The various flap deflections were obtained by means of separate flap inserts, which were contoured to correspond to the profile of the deflected flap and wing. (See fig. 2.) Thus, the flaps were investigated for a sealed-flap condition.

The fuselage of the model was evolved from a body of revolution of fineness ratio 11. The addition of the canopy and bulging in the vicinity of the wing-body juncture, necessary to enclose the power plants, together with termination of the body at the exit of the tail pipe, reduced the effective fineness ratio to 8.5. For the present investigation the engine ducts were sealed and faired smoothly into the fuselage. Listed below are some geometrical characteristics of the model:

Aspect ratio	2.50
Taper ratio0385
Airfoil section (streamwise).	(See fig. 2.)
Total wing area, S, square feet	1.406
Mean aerodynamic chord, \bar{c} , feet	0.800
Dihedral, degrees	-5
Incidence, degrees	0



The model was constructed entirely of steel. All exposed surfaces of the model were unpainted and polished smooth.

Scope of Experimental Data

The lift, drag, and pitching moment of models having either the round- or sharp-leading-edge wings with zero flap deflection were obtained at Mach numbers of 0.60, 0.80, 0.90, 1.35, 1.45, 1.60, and 1.90 at a constant Reynolds number of 3.0 million. Corresponding data were obtained for the model with the round-leading-edge wing for flap deflections of -3° and -6° , and for the model with the sharp-leading-edge wing for a flap deflection of -3° .

Other control surfaces, such as rudder, elevators, ailerons, and trailing-edge flaps, remained undeflected throughout the present investigation.

Corrections to Data

The various corrections applied to the data, which were of the same magnitude for all configurations, account for the following factors:

1. Induced effects of the tunnel walls at subsonic speeds resulting from lift on the model. The magnitudes of these corrections which were added to the uncorrected results were as follows:

$$\Delta\alpha = 0.315C_L, \text{ deg} \quad \Delta C_D = 0.0055C_L^2$$

2. Change in the velocity of the air stream in the vicinity of the model at subsonic speeds due to constriction of the flow by the tunnel walls. At a Mach number of 0.90, this correction amounted to about a 2-percent increase in the Mach number over that determined from a calibration of the wind tunnel without a model in place.

3. The longitudinal force experienced by the model body due to the streamwise variation of static pressure as measured in the test section at subsonic and supersonic speeds without a model in place. This correction varied from as much as -0.0026 at a Mach number of 1.35 to 0.0036 at a Mach number of 1.70.

The drag coefficients as presented herein are in essence only fore-drag coefficients since the data have been adjusted to correspond to those in which the base pressure would be equal to the static pressure of the free stream. In addition it should be noted that, since the engine inlets

were sealed, the drag data as presented do not include any drag due to air flow through the ducts.

Results of tests of each model, with undeflected flaps, to determine the effective stream angle, indicate that a stream angle of about -0.1° exists at both subsonic and supersonic speeds. No correction was made to the data of the present report to account for this effect.

RESULTS

The results of the present investigation are presented graphically in figure 3. The effects of flap deflection and of flap nose shape upon the variation of several aerodynamic parameters with Mach number are presented in figures 4 and 5, respectively.

The results of the present investigation indicate that deflection of the leading-edge flaps, having either a round or sharp leading edge, had the following effects:

1. The variations of lift with angle of attack and of pitching moment with lift near zero lift were not significantly affected. (See fig. 3.)
2. In general at all test Mach numbers, the drag at zero lift increased with flap deflection. (See figs. 3 and 4(a).)
3. The maximum lift-drag ratio was increased at subsonic speeds, and the increment in the maximum lift-drag ratio for a given flap deflection decreased as the Mach number approached unity. At supersonic speeds, flap deflection had no influence upon the maximum lift-drag ratio. (See fig. 4(b).)

The results of the present investigation indicate that rounding the wing leading edge, and consequently the flap nose shape, did not change the lift, drag, or pitching-moment characteristics of the model (see figs. 3 and 5), except that at $M = 1.90$ rounding the leading edge increased the drag at zero lift.

Ames Aeronautical Laboratory
National Advisory Committee for Aeronautics
Moffett Field, Calif., Feb. 16, 1954

FIGURE LEGENDS

Figure 1.- Projected views of model and model dimensions.

Figure 2.- Airfoil section of each wing and sketch of flap insert.
(a) Airfoil sections of each wing. (b) Detail of flap insert.

Figure 3.- Effect of flap deflection upon the aerodynamic characteristics of each model at various Mach numbers; $R=3.0$ million. (a) $M=0.60$

Figure 3.- Continued. (b) $M=0.80$

Figure 3.- Continued. (c) $M=0.90$

Figure 3.- Continued. (d) $M=1.35$

Figure 3.- Continued. (e) $M=1.45$

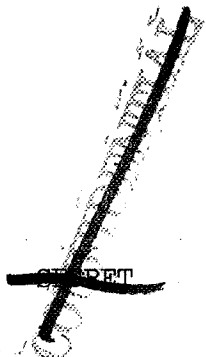
Figure 3.- Continued. (f) $M=1.60$

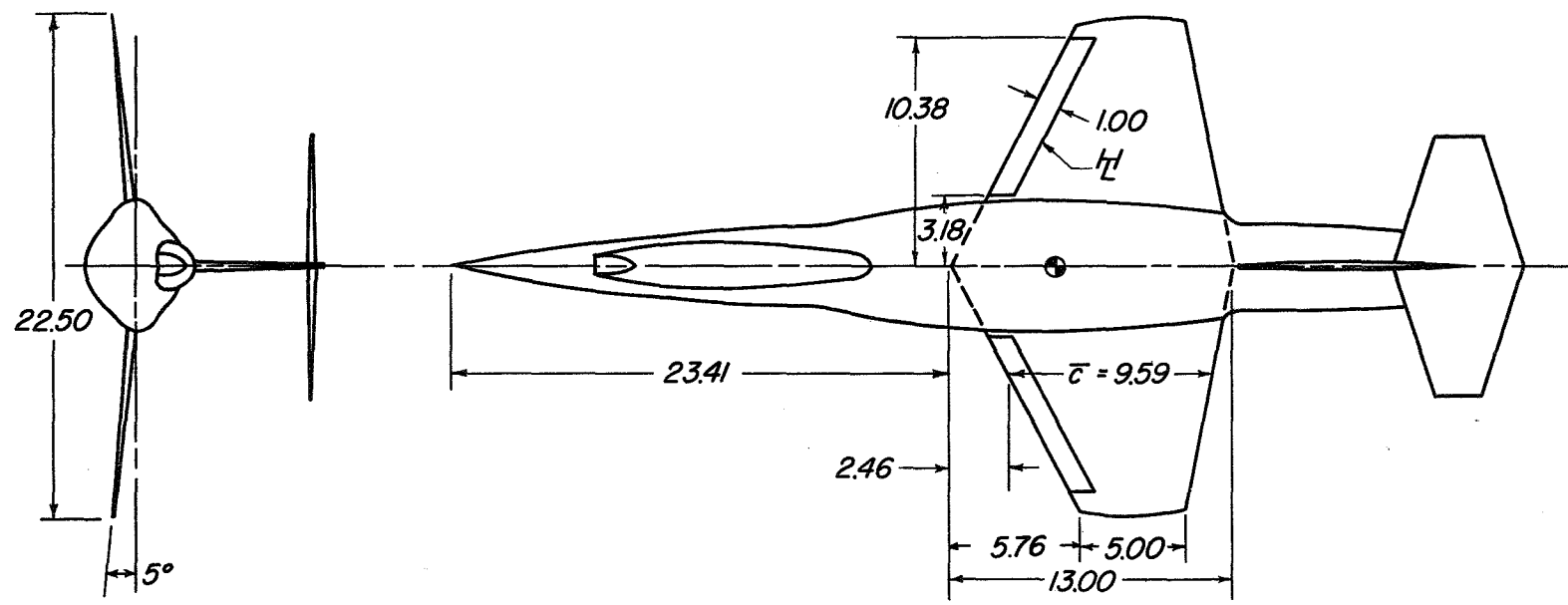
Figure 3.- Concluded. (g) $M=1.90$

Figure 4.- Effect of flap deflection upon the variation with Mach number of the drag at zero lift and maximum lift-drag ratio of each model; $R=3.0$ million. (a) $(C_D)_{L=0}$ vs. M

Figure 4.- Concluded. (b) $(L/D)_{max}$ vs. M

Figure 5.- Effect of nose shape upon the variation with Mach number of several aerodynamic characteristics; $R=3.0$ million.





All dimensions shown in inches
unless otherwise noted

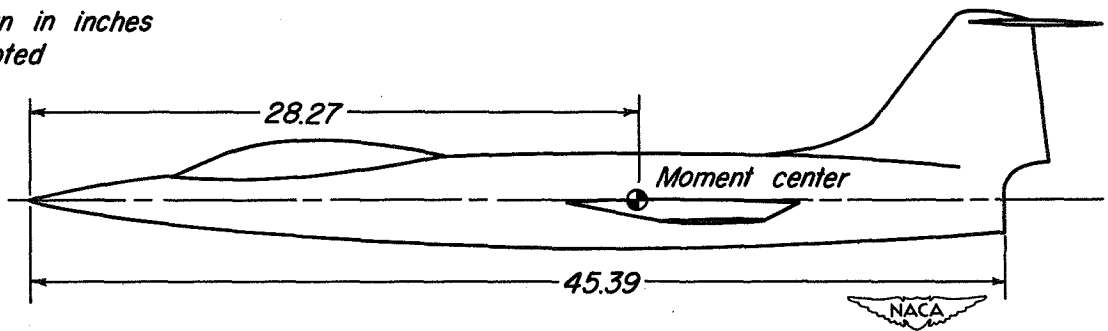
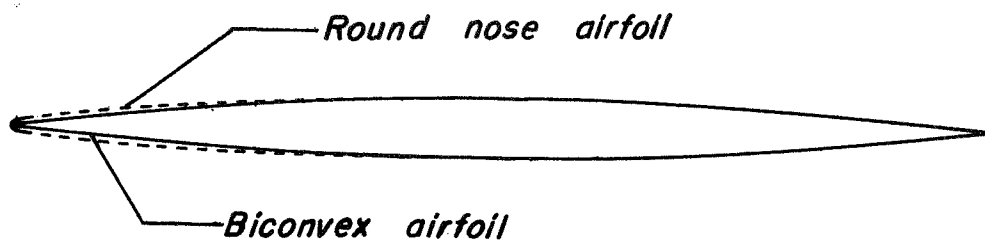
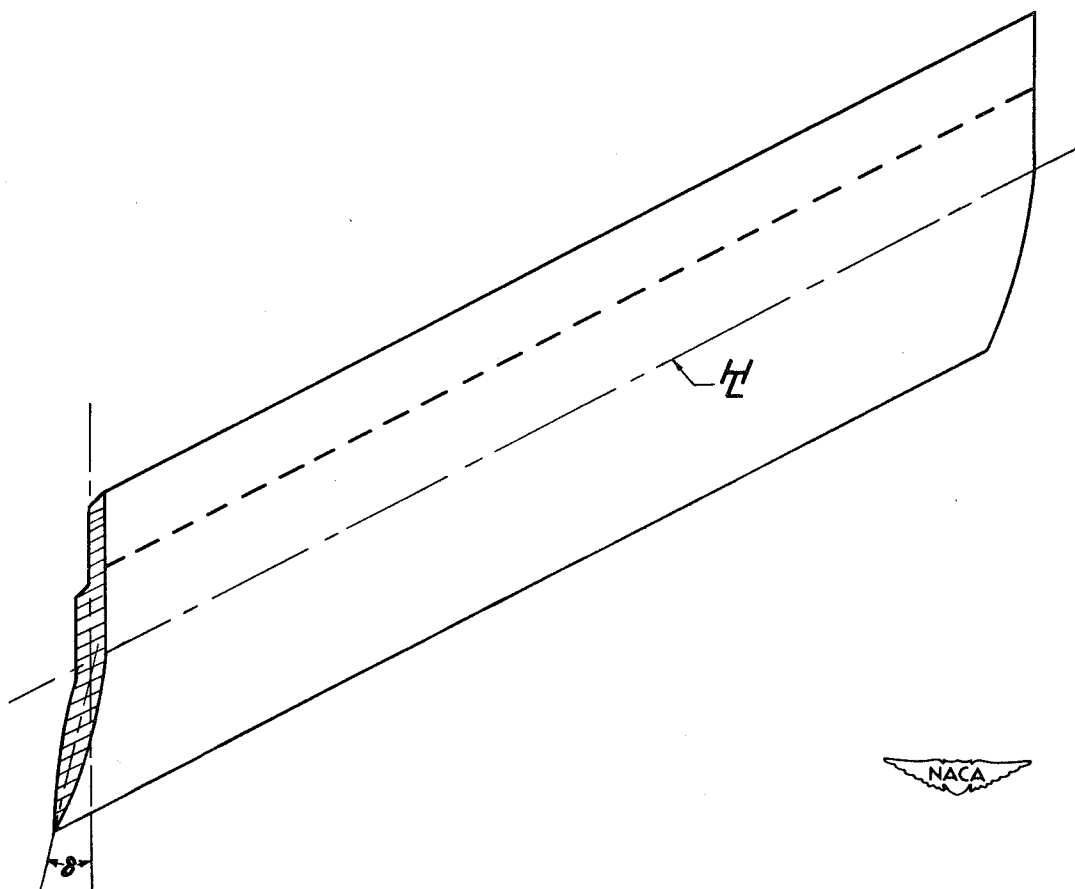


Figure 1.- Projected views of model and model dimensions.



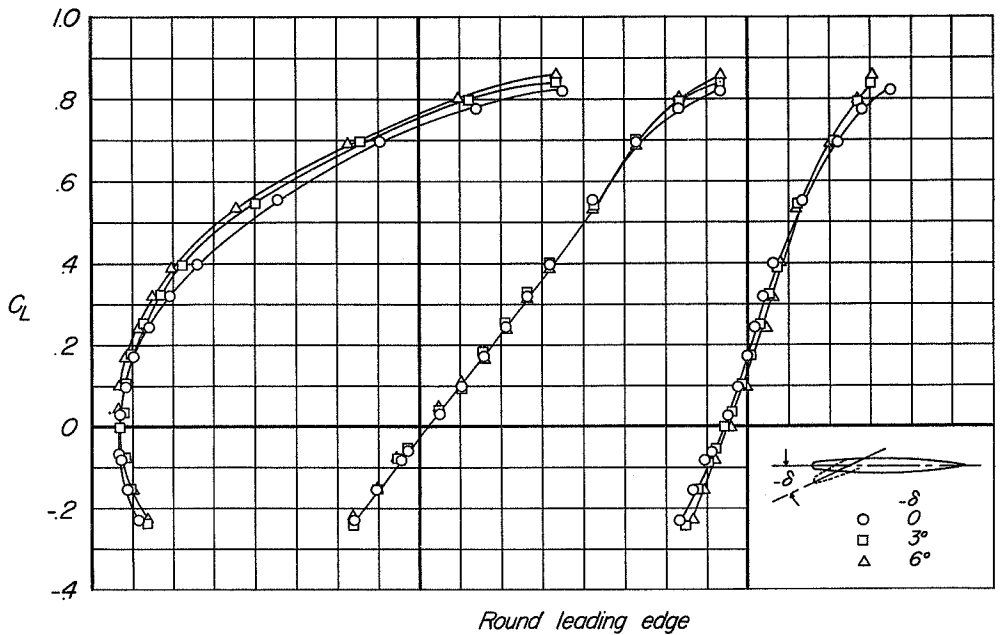
(a) Airfoil sections of each wing.



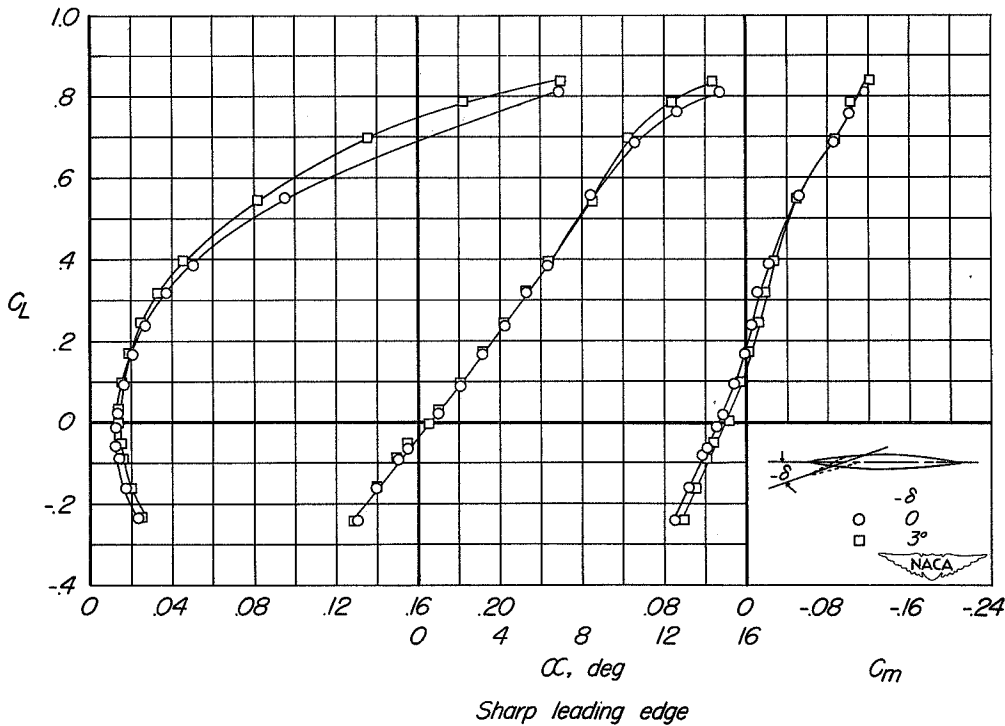
(b) Detail of flap insert.

Figure 2.- Airfoil section of each wing and sketch of flap insert.





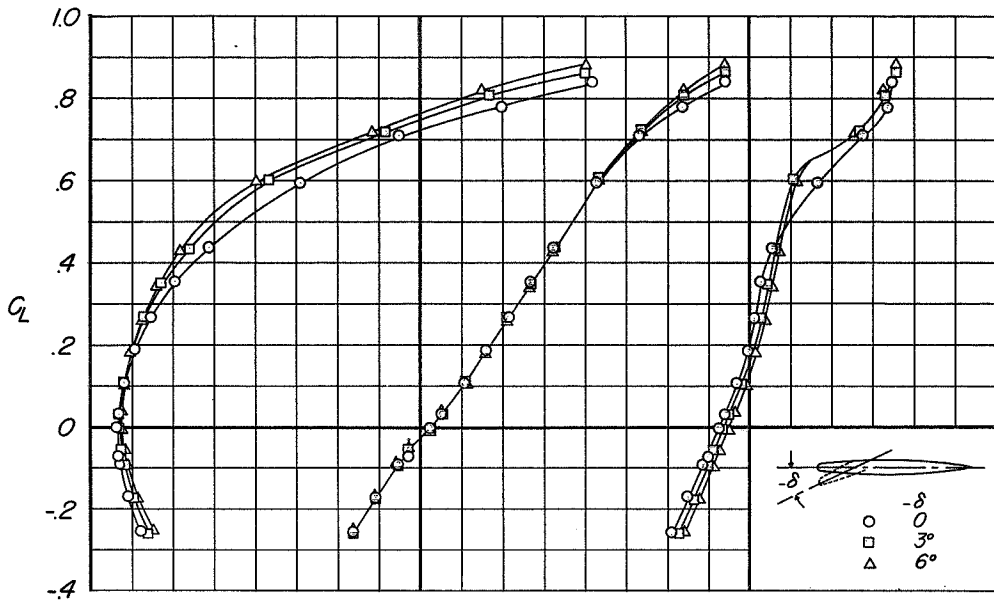
Round leading edge



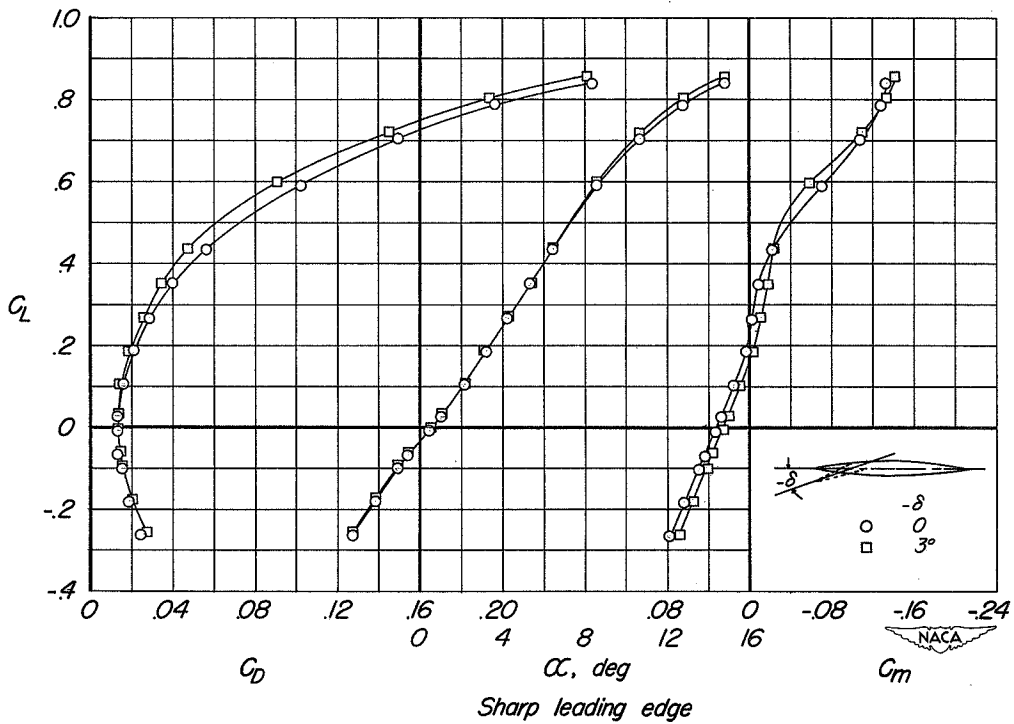
Sharp leading edge

(a) $M=0.60$

Figure 3.- Effect of flap deflection upon the aerodynamic characteristics of each model at various Mach numbers; $R=3.0$ million.



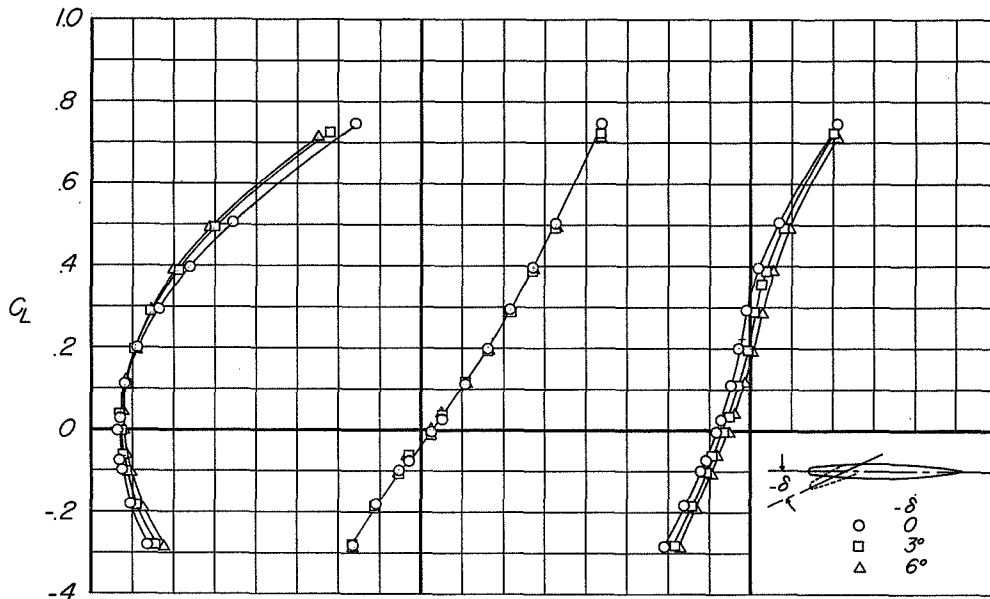
Round leading edge



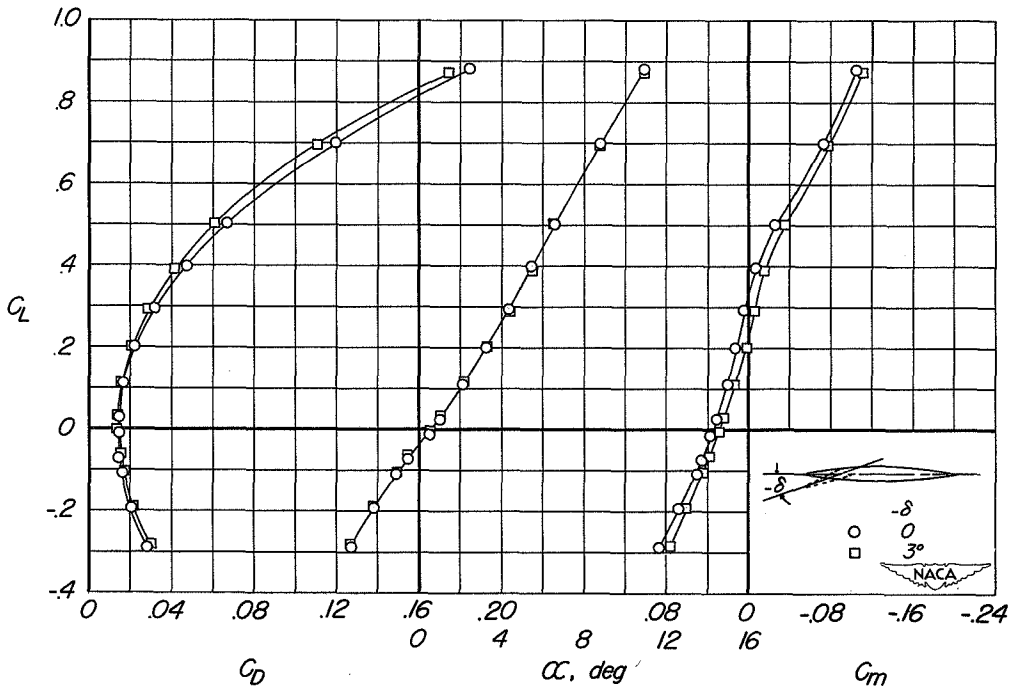
Sharp leading edge

(b) $M=0.80$

Figure 3.- Continued.



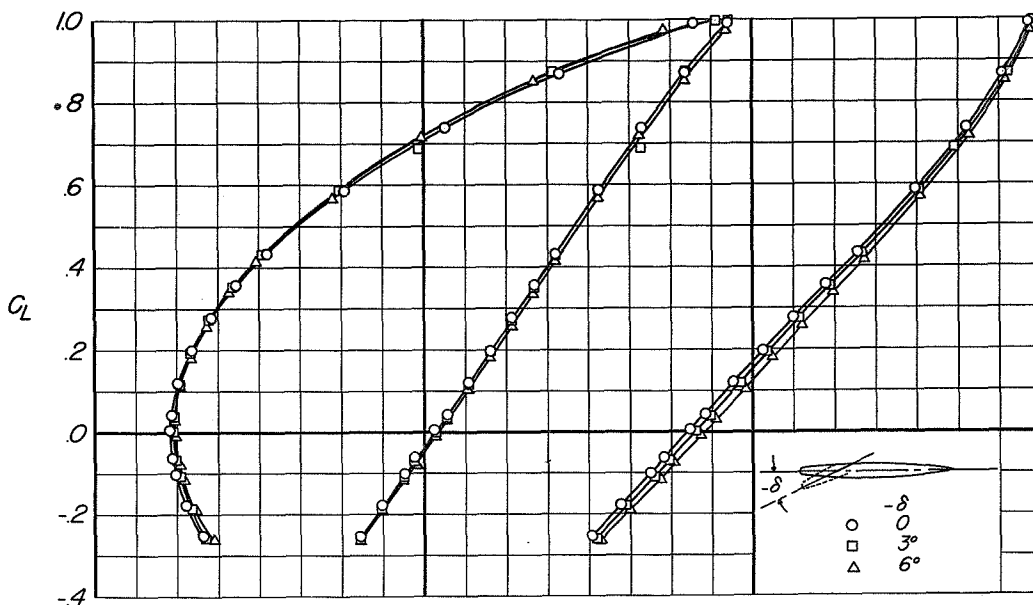
Round leading edge



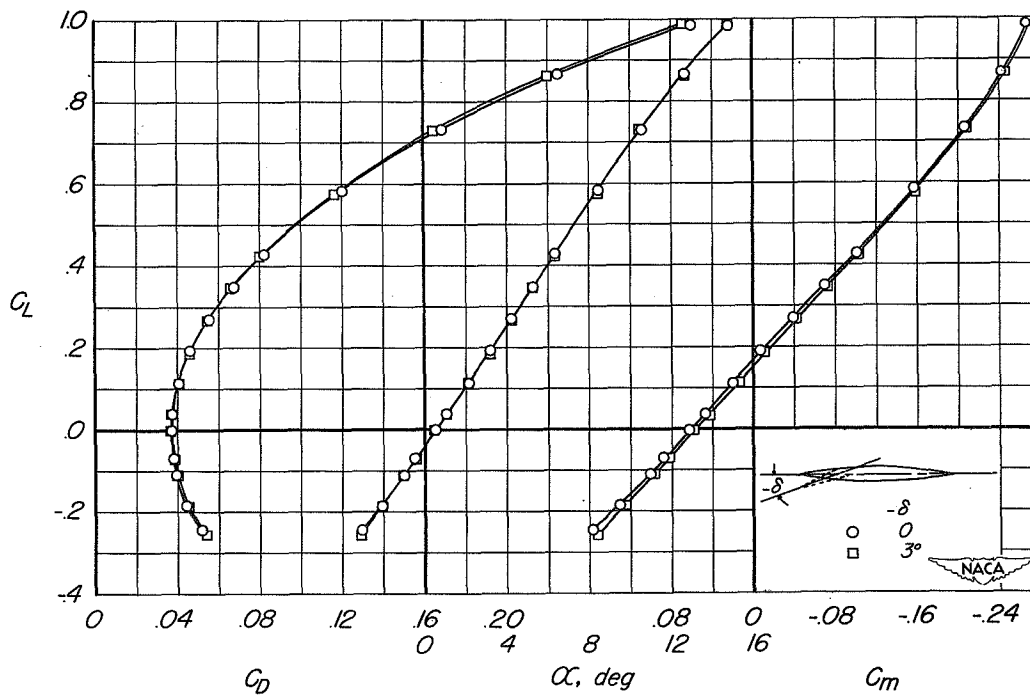
Sharp leading edge

(c) $M=0.90$

Figure 3.- Continued.



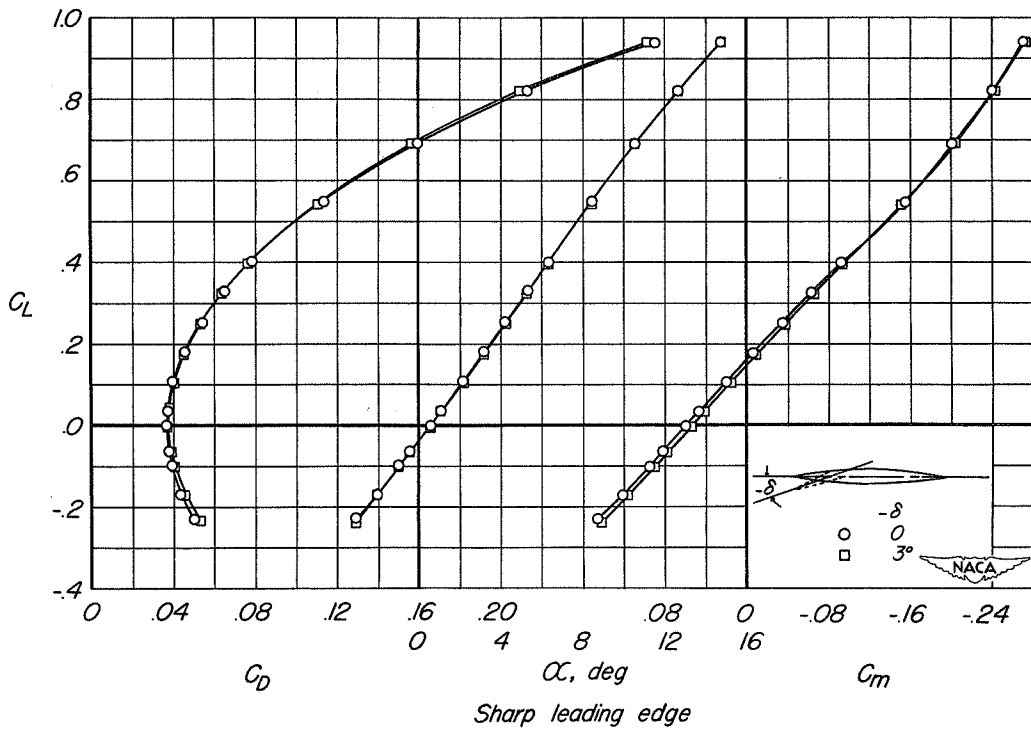
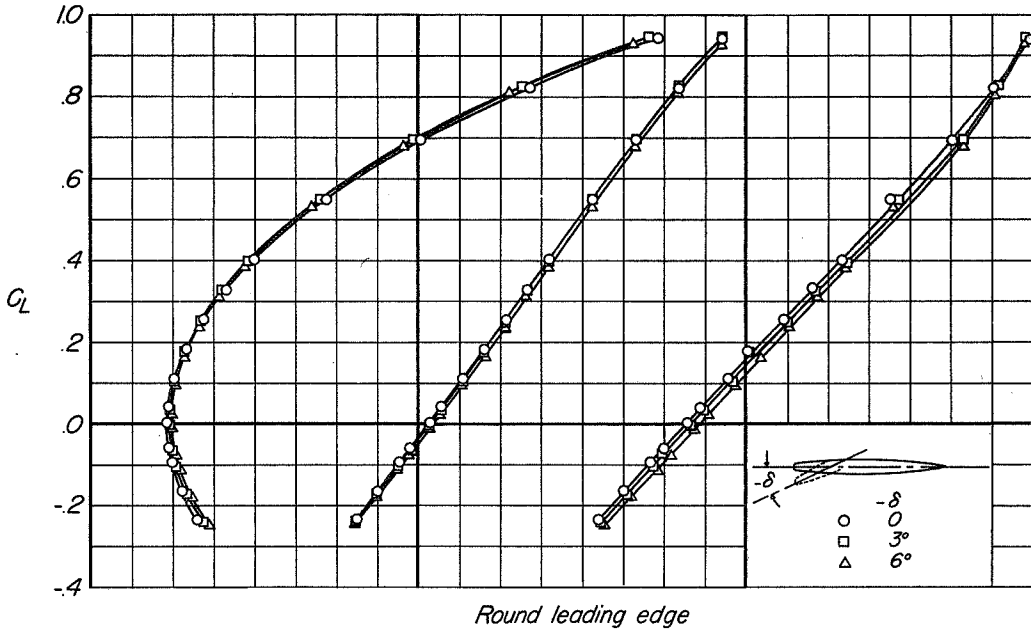
Round leading edge



Sharp leading edge

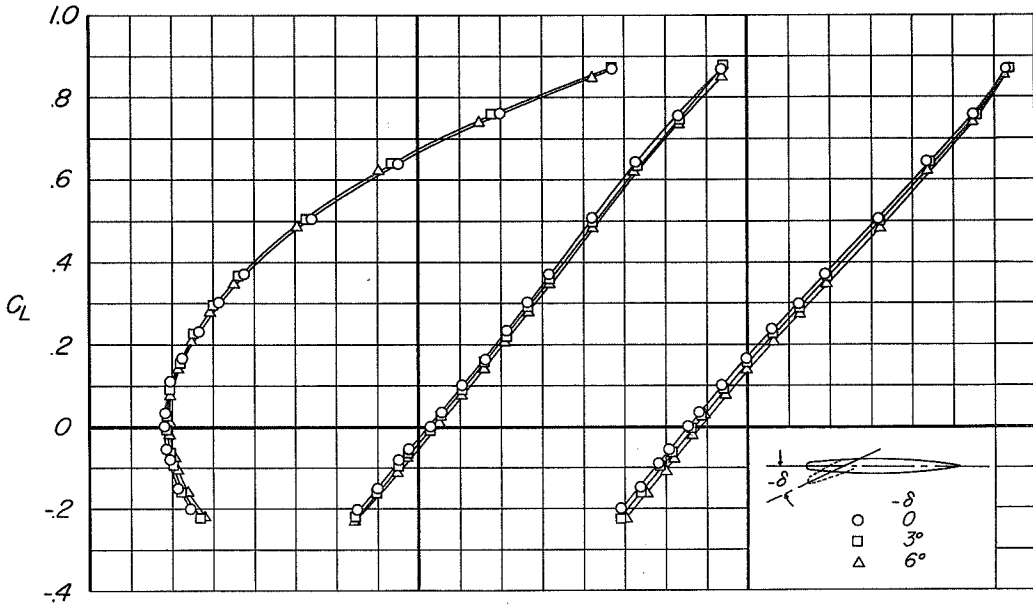
(d) $M=1.35$

Figure 3.- Continued.

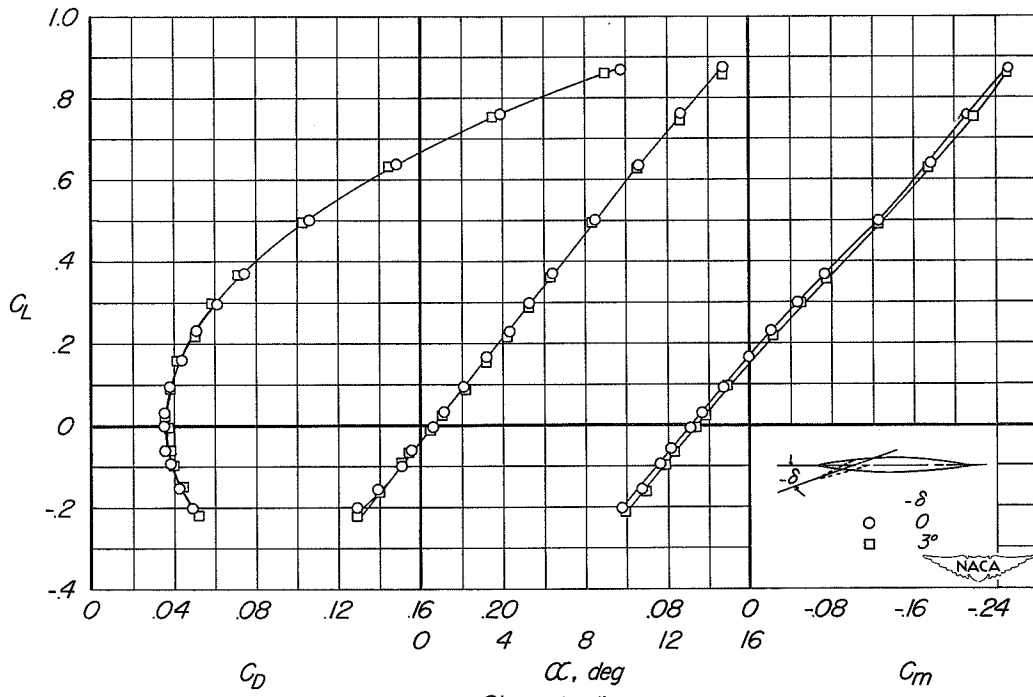


(e) $M=1.45$

Figure 3.- Continued.



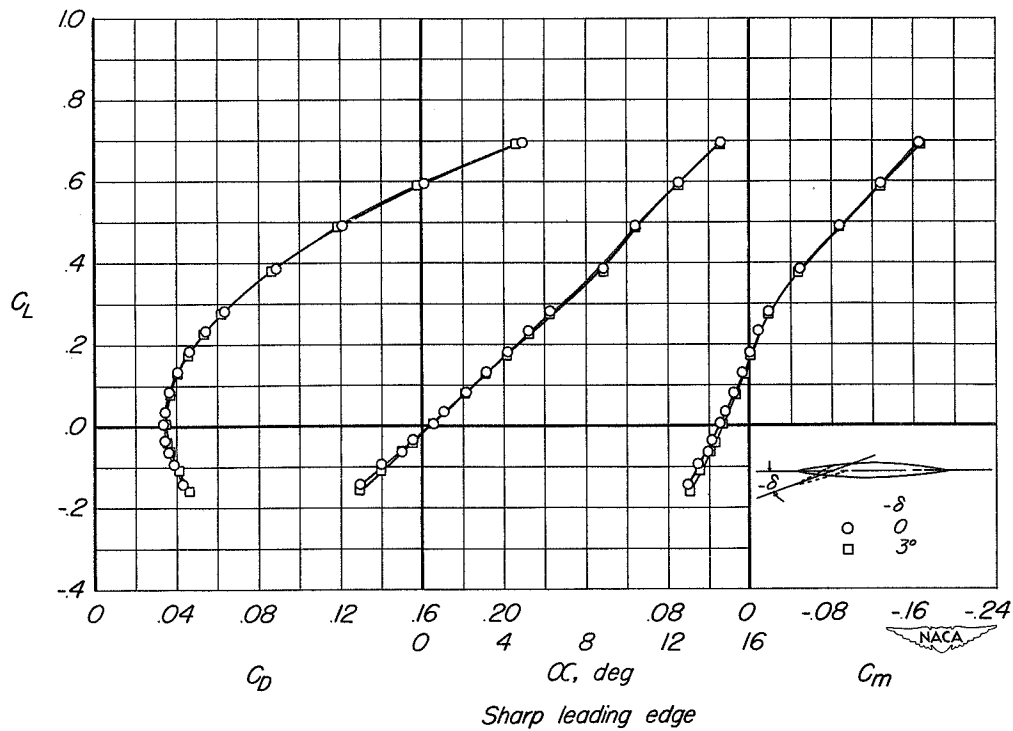
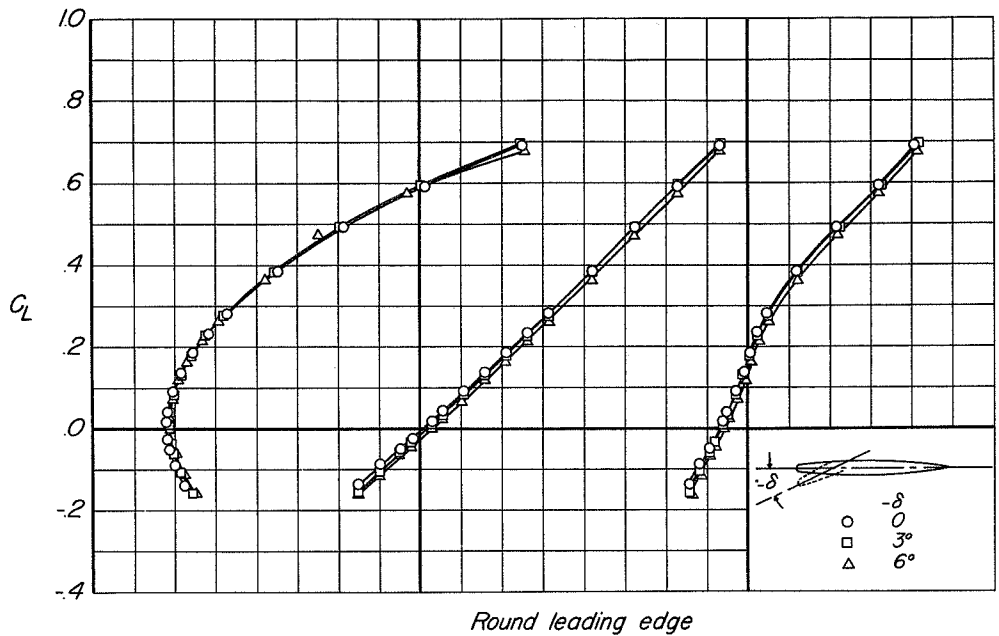
Round leading edge



Sharp leading edge

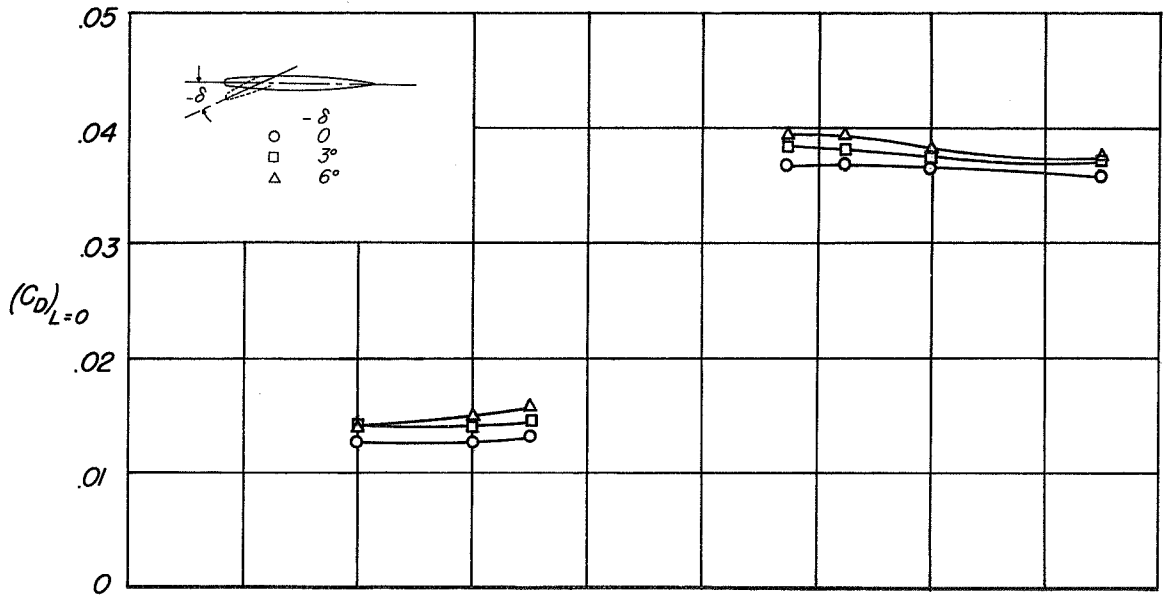
(f) $M=1.60$

Figure 3.- Continued.

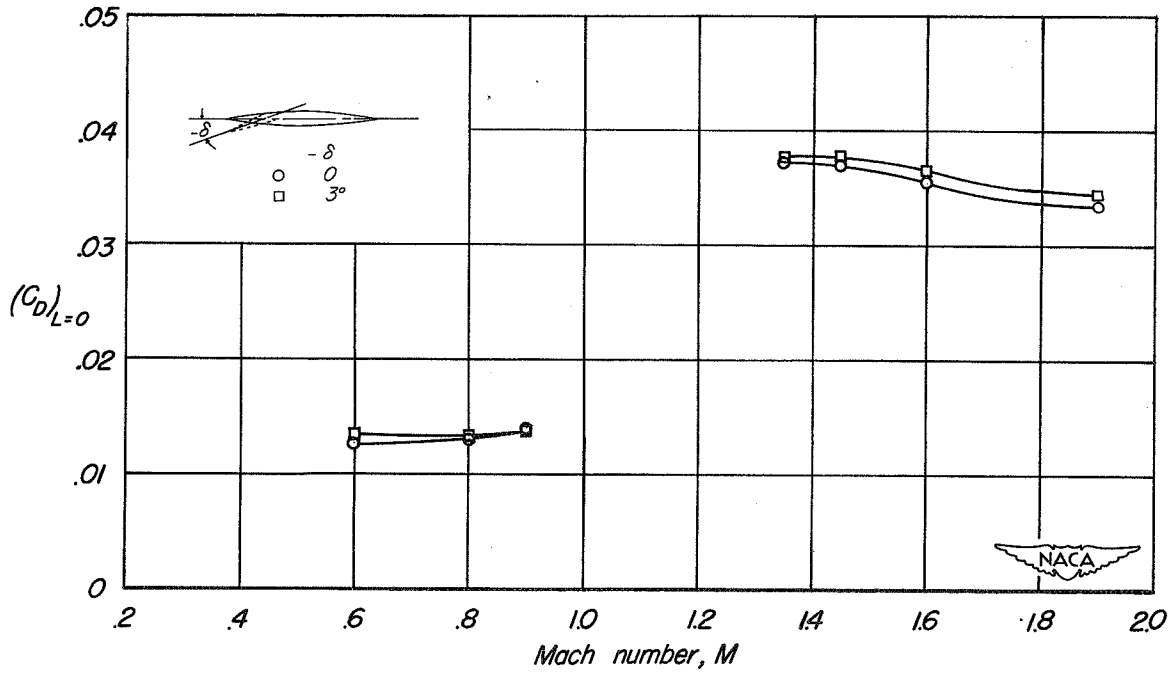


(g) M=1.90

Figure 3.- Concluded.



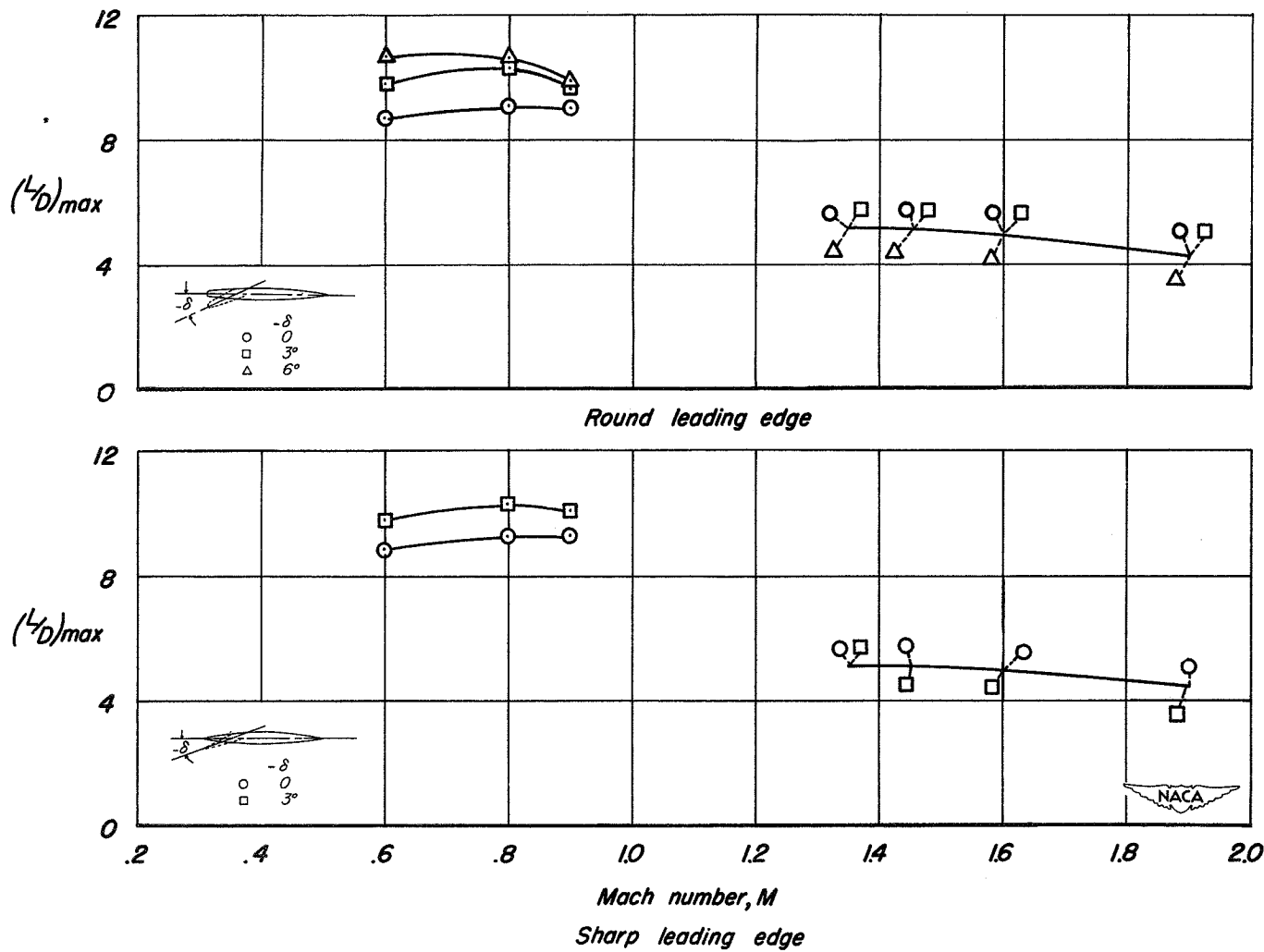
Round leading edge



Sharp leading edge

(a) (C_D)_{L=0} vs. M

Figure 4.- Effect of flap deflection upon the variation with Mach number of the drag at zero lift and maximum lift-drag ratio of each model; R=3.0 million.



(b) $(L/D)_{max}$ vs. M

Figure 4.- Concluded.

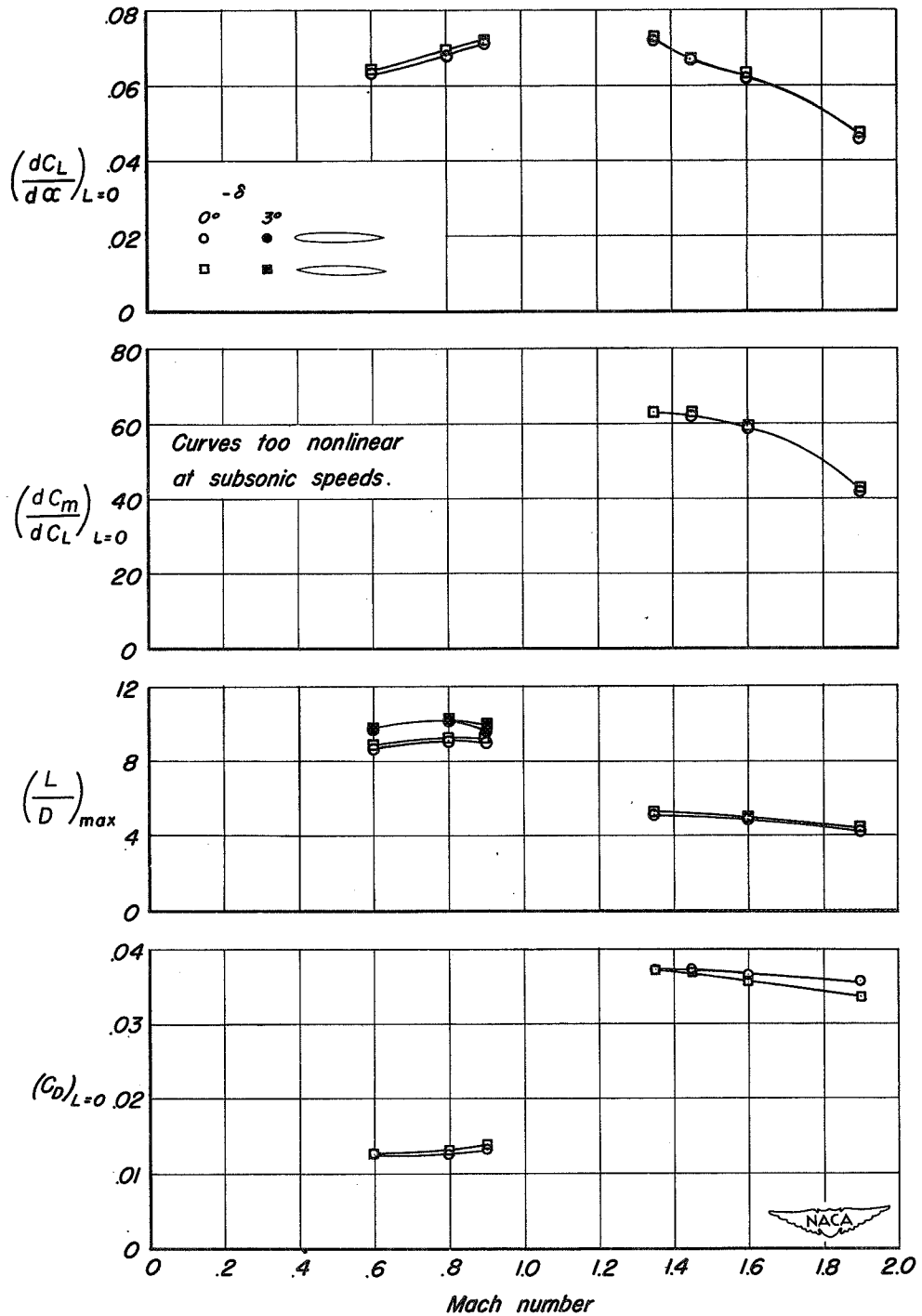


Figure 5.- Effect of nose shape upon the variation with Mach number of several aerodynamic characteristics; R=3.0 million.